ENGINOM | Engineering Innovations

Available online at www.enginom.org
ENGINOM in Engineering Innovations
(E-ISSN: xxxx-xxxx; ISSN: xxxx-xxxx)
Vol. 1, No. 01, March, 2026

The flexural behavior of RC beams strengthened by near-surface mounted steel or FRP bars is investigated experimentally and numerically

Article,

A. Ali [1, *]

1 Department of Civil Engineering, Higher Technological Institute, 10th of Ramadan City 44629, Egypt; Ahmed.ali@hti.edu.eg,
* **Corresponding author**: A. Ali, ;

Academic Editor:
Abd Al-Kader A. Al Sayed

Submission: 22 April 2026
Revision: 27 April 2026
Acceptance: 30 April 2026

Citation: To be added by editorial staff during production.

Abstract

The near-surface mounted (NSM) method, which involves attaching strips or rods in grooves made inside the concrete cover with an adhesive, has been shown to be efficient in strengthening because of the bonding area it offers and its capacity to delaying debonding. The flexural behavior of reinforced concrete (RC) beams strengthened with steel and fiber reinforced polymer FRP bars was experimentally investigated. Four RC beams were casted and tested under four points loads. The effect of bars types was studied represented in steel, glass-FRP (GFRP), and carbon-FRP (CFRP). The load capacity, deflection, failure modes, crack patterns, stiffness, toughness, and ductility of the tested RC beams were collected and analyzed. Enhancing for beam strengthened with NSM steel, GFRP, and CFRP bar in carrying load with 60.6, 72.6, and 81.1% and in yielding loads 78.1, 45.3, and 82.8% respectively over the control beam (CB).

Keywords: Near-surface mounted; CFRP; GFRP; Strengthening; Failure modes; Crack patterns.

1. Introduction

Degradation of concrete and steel corrosion of reinforcement concrete (RC) structures raised the concerns about structural efficiency. Retrofitting or strengthening of such RC structures has become urgent and important to maintain or upgrade their performance by using various methods [1], [2], [3]. These methods involve externally bonded (EB) by bonding plates from steel or fiber-reinforcement polymer (FRP) at the tension side of the strengthened beams, NSM, where the reinforced bars or strips are inserted into slits made inside the concrete cover, and using ultra high-performance concrete (UHPC) strips [4], [5]. Using NSM proven to be more effective than others strengthening techniques due to its several advantages which are presented in less installation time, improved bond capacity, and post-strengthening protection [6], [7]. Although, there is still little knowledge on how NSM-FRP bars bond to concrete [8], [9].

Bilotta et al. [1] studied the flexural behavior of RC beams strengthened with both NSM and EBR techniques. The result showed that strengthening using NSM with fewer CFRP strips had more load carrying capacity more than those strengthening with EB strips [1], [10]. This conclusion has been verified by M.H. Seleem [11], [12], [13] through numerical and research on RC beams reinforced with high-strength concrete reinforced with EB and NSM. The result indicated that strengthening using NSM increase the load capacity by 147.9% to 172.0% compared to the control beam by using steel RHSC layer and GFRP bars respectively [11], [12], [13]. However, these ratios are much higher than those with EB RHSC layers due to the

accelerated debonding failure [5], [14]. This is consistent with, who reported that beams strengthened with NSM strips had a greater capacity load than beams reinforced with EBR in the same FRP area [15], [16], [17]. The ultimate load of NSM beams reinforced was 12–18% greater than that of EB-reinforced beams [18], [19], [20]. In showed that while the EB CFRP sheet is more suited for severely damaged corbels, the NSM steel bars technology might be used as an acceptable approach in the early stages of damage [4], [21]. Also statics and dynamic tests have proven the superiority of NSM technique over the EB system in improving the stiffness of strengthened beams [22], [23], [24].

Eight RC beams were tested by I.A. Sharaky et al. [5], [6], [11] to examine how strengthened beams with NSM behaved with different kinds of FRP, Furthermore, the CFRP and GFRP strengthened beam exceeded the control beam capacity by 166.3 and 159.4%, respectively, it also recorded that the beam strengthened with CFRP bars experienced higher stiffness. And it was noted that the concrete cover separation (CCS) failure mode controlled the ultimate capacity load [4], [25], [26]. The impact of the interaction between the NSM strips and the strengthened members' primary reinforcement was examined in and the result showed that installation NSM GFRP strips side by side in one groove has a lower interfacial stress than those installed into two grooves separated and increasing the grooves depth to install the NSM-GFRP strips near the stirrups can delay the cover separation and increase the ultimate load about 1.5 time that installed near the bottom surface of the beam. Also, El-Gamal et al. [9], [27] discovered the ability to increase the final capacity of the strengthened beam by almost 85% by doubling the FRP area. Moreover, in the experimental results showed that the possibility of improving the initial stiffness of 58- 71%, and energy absorption of 35- 96% for the GFRP-retrofitted beams compared to the control beam [28], [29], [30]. Not only the bottom cover of the RC beam in the only place to installation the NSM bar, but it can be possible to install at the side cover but with lower load-carrying capacity and flexural stiffness [31], [32], [33].

Wei sun et al. [34], [34] developed an anchored system to fully NSM-FRP bond and increase the FRP tensile strength up to rupture. While, others bent the end of GFRP-NSM bars by different angles equal to 0º, 45º, and 90º to delay the failure of concrete cover separation and the NSM-bar debonding [35], [36], [37]. The result indicated that the end anchors delayed the CCS and increases the ultimate load by 201% over the control beam while straight bars increase the ultimate load up to 177% [29], [38], [39]. While Rahulreddy [40] increased the ultimate capacity and strengthened the connection between NSM-FRP bars by using EB U-wrap FRP and convert the failure mode to NSM-FRP bar rupture. In addition to using mechanical interlocking grooves or by use anchored technique with the prestressed can delay the CCs and enhancing the carrying load [12], [41], [42]. As, Hesham M.A. Diab and T. Abdulaleem [43], [44] proved that using NSM FRP rods and embedded through-section ETS anchors demonstrated greater ductility and bond strength than face-to-face connections.

In the present study, the effectiveness of strengthening RC beams by several types of NSM bars including steel, GFRP, and CFRP bars. A total of four beams including the control beam tested up to failure under four points loads. Carrying capacity load, failure mode, stiffness and load-deflection behavior were analyzed.

1.1. Research Significance

The deterioration of reinforced concrete (RC) infrastructure due to aging, corrosion, increased service loads, or design flaws necessitates effective and reliable strengthening solutions. Among various retrofitting techniques, the Near-Surface Mounted (NSM) method has emerged as a superior alternative to externally bonded reinforcement (EBR), offering better bond characteristics, improved protection against environmental exposure, and higher ultimate load capacity. However, the selection of the optimal NSM reinforcement material—

conventional steel versus advanced Fiber-Reinforced Polymer (FRP) composites—remains a critical engineering decision with significant implications for structural performance, cost, and long-term durability.

The primary significance of this research lies in its **comprehensive comparative analysis** of NSM steel and FRP bars, addressed through a novel integration of full-scale experimental testing and validated numerical modeling. While previous studies have investigated NSM strengthening using either steel or FRP independently, a direct, systematic comparison under identical boundary and loading conditions is notably lacking. This study fills that gap by providing critical insights into the distinct flexural failure mechanisms, load-deflection responses, ductility, and crack propagation patterns associated with each material.

Specifically, the research significance is threefold:

1. **Bridging the Gap between Strength and Ductility:** FRP bars offer high tensile strength and corrosion resistance but are linear-elastic until brittle failure, raising concerns about sudden collapse. Steel bars, while ductile, are susceptible to corrosion and heavier. This study quantifies the trade-offs, offering engineers evidence-based guidance on selecting the appropriate NSM material based on performance objectives (e.g., maximizing strength vs. maintaining ductility and warning signs before failure).
2. **Development and Validation of a Robust Numerical Framework:** A major contribution is the creation and calibration of a detailed finite element (FE) model that accurately simulates the complex bond-slip behavior at the NSM bar-epoxy-concrete interface for both steel and FRP. This validated numerical tool transcends the specific tested beams, enabling future parametric studies (e.g., varying bar diameter, bond length, concrete strength, or number of NSM bars) without costly and time-consuming experiments. It serves as a predictive platform for optimizing strengthening designs.
3. **Practical and Economic Implications:** By directly comparing the flexural performance of NSM steel bars (a readily available, lower-cost, but heavier material) against NSM FRP bars (a higher-cost, lightweight, corrosion-resistant alternative), this research delivers actionable data for infrastructure owners and designers. The findings help justify initial material costs against long-term maintenance, life-cycle costs, and structural safety, particularly for applications in aggressive environments or for structures requiring minimal dead-load increase.

Ultimately, this research advances the state-of-the-art in structural retrofitting by moving beyond isolated material studies to a holistic, comparative, and validated understanding. The combined experimental and numerical approach not only enhances the reliability of current design recommendations but also accelerates the adoption of rational, performance-based selection criteria for NSM strengthening systems, leading to safer, more durable, and cost-effective reinforced concrete structures.

2. Methodology

2.1. Tested RC beams

The bending capacities of four reinforced concrete (RC) beams in a four-point loading configuration were evaluated. Each sample was a rectangular cross-section with dimensions of 160 mm for width, 280 mm for height, 2400 mm for total length, and 2200 mm for clear span, as indicated in **Error! Reference source not found.**. The specimens were designed in accordance with ACI 440.1R-15. The bottom concrete cover was 30 mm and 15 mm from all other sides. Two ribbed steel bars with 10 mm diameter were used for upper and lower inner reinforcement with 0.0035% bottom reinforcement ratio. And to exclude shear failure 8 mm diameter smooth steel stirrups used with spacing 100 mm uniformly distributed along the

length of the beam expect the shear span which was without any stirrups three tested beams in this study were strengthened with NSM steel bars, GFRP bars, and CFRP bars with the same diameter of 12 mm as indicated in **Error! Reference source not found.** while one beam was kept un-strengthened (CB) to investigate how NSM material affects beam response.

2.2. Material properties

2.2.1 Concrete

Ready-mixed concrete was used to cast all tested beam with average concrete compressive strength 28 MPa were obtained after testing six cylinders (150 x 300) mm after 28 days according to ASTM C469-87. The mixture comprised 350 kg/m^3 of ordinary Portland cement, 650 kg/m^3 of sand, 1200 kg/m^3 of crushed dolomite, a water-to-cement ratio of 0.40, and a superplasticizer amounting to 0.2% of the cement weight.

2.2.2 Steel Reinforcement

In order to determine the yielding and ultimate stress of the inner steel reinforcement, the steel using in strengthening and the mild steel for stirrups, three samples were tested for each type based on UNE-EN ISO 15630-1. The Younge's modulus for all steel was 200 GPa. The longitudinal reinforcement consisted of bars with a nominal diameter of 10 mm, used for both tension and compression with stress strain curve shown in **Error! Reference source not found.**. While mild steel with 8 mm nominal diameter was used for stirrups with 100 mm spacing.

2.2.3 FRP bars and adhesive material

The NSM-FRP bars (GFRP and CFRP) bars properties were obtained under tensile test based on ACI 440.3R-12 after fixing a 300 mm steel tube glued at the two ends of the tested bar. **Error! Reference source not found.** and **Error! Reference source not found.** indicate the bar characteristics experimentally obtained from tensile tests. A two-component epoxy (Sikadur-31CF) with 35 MPa tensile strength was used to bond the strengthened bars to concrete.

2.3 Preparing and casting of samples

The reinforcement steel cages for each specimen weas firstly prepared and placed in a wood framework and fixed using small mortar blocks with height 30 mm to ensure the bottom cover distance **Error! Reference source not found.**.b and to easily formed the NSM groves, especially foam stick with dimension similar to the grooves size were placed at the tension side of the beam before casting. all grooves were (20x20) mm chosen according to ACI-440.2R,2008. After the concrete casting the NSM bar was inserted using Sidadure-31CF (**Error! Reference source not found.**c).

2.4 Set-up and instrumentation

All beam instrumentations are shown in **Error! Reference source not found.**. to determine the deflection through the length of the all beams, three vertical transducers (LVDTs) were used at the mid-span and under the two loads. Strain gauges were attached to the inner steel reinforcement and the NSM bars at the midspan with 6 mm gauge length to measure the strains values during the test. and other strains with 60 mm gauge length were utilized at the upper compression zone of the tested beam to measure the compression strain of the concrete. To test under four-point load, the loads from the 1000 kN hydraulic jack were distributed using a steel spreader beam as shown in **Error! Reference source not found.**. All data were collected by an automatic data acquisition system.

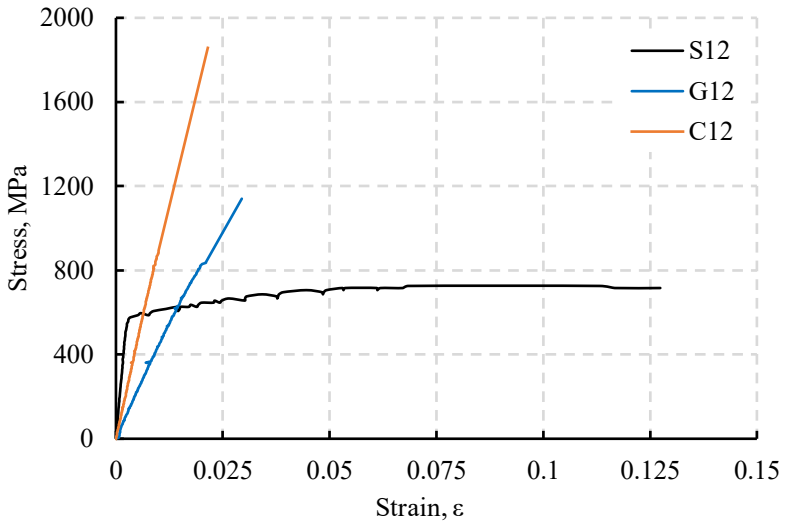

Figure 1. The stress-strain curves for steel, FRP, and hybrid bar.

Table 1. Configuration of the experimentally tested beam

Beam ID	No. of strengthened bar	End Condition	Test variable
CB	--	--	CB
S1S	1 steel	Straight end	Bar material
S1G	1 GFRP	Straight end	Bar material
S1C	1 CFRP	Straight end	Bar material

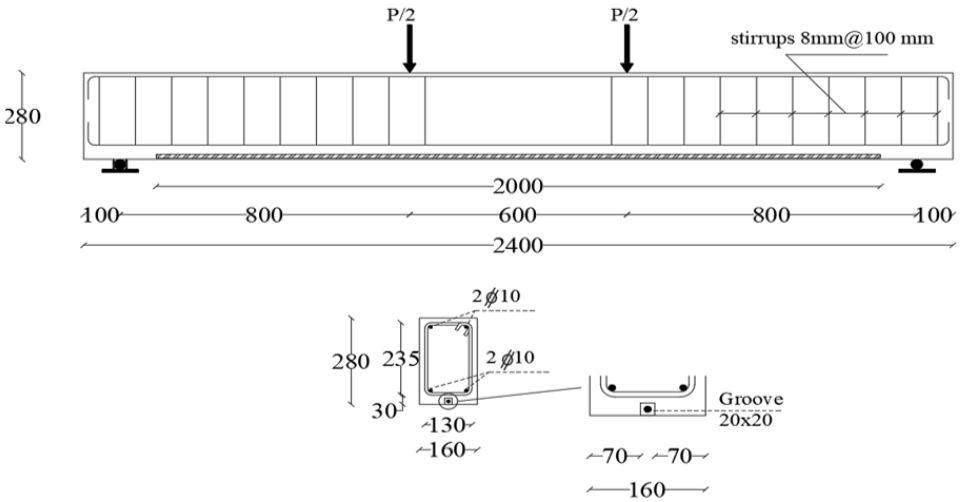

Figure 2. Beam dimension and details of the grooves

(a) (b) (c) (d)

Figure 3. Specimen preparation and NSM bar inserting, (a) Framework preparation, (b) Steel cage, (c) Inserting the NSM bar and (d) Filling extra epoxy

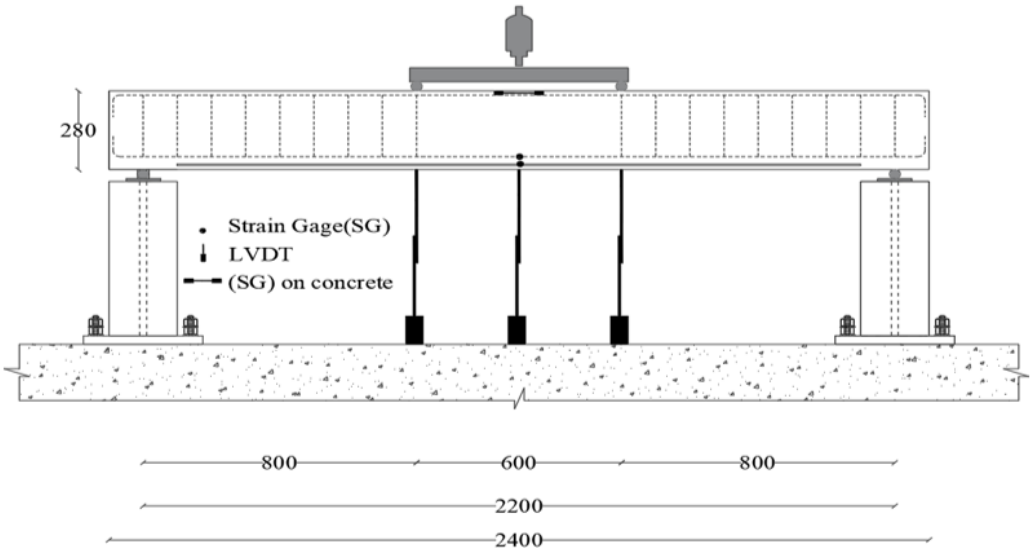

Figure 2. Beam dimension and details of the grooves

Figure 3. Setup and instrumentation

3. Results and discussions

3.1. Uniaxial tensile stress-strain of steel and FRP bars

The steel bar recorded yield stress, ultimate stress, and the modulus of elasticity (MOE) of were 520 MPa, 726.2MPa, and 212 GPa respectively, while the GFRP bar and CFRP bar recorded an ultimate load 1140.7 MPa and 1857.4 MPa and MOE of 51 GPa and 92 GPa respectively (**Error! Reference source not found.** and **Error! Reference source not found.**).

Table 2. Properties of steel, FRP, and hybrid bars

Bar ID.	Steel core dia. (mm)	Outer dia. (mm)	FRP material	Bar Materials	Fu (MPa)	E (GPa)
S12	--	12	--	Steel	726.2	212.0
G12	--	12	GFRP	GFRP	1140.7	51.0
C12	--	12	CFRP	CFRP	1857.4	92.0

3.2. Load capacity, Failure mode, and Cracking behavior

As shown in **Error! Reference source not found.**-the control beam (CB), and beam with one steel strengthened bar (S1S) failed due to flexural failure by concrete crushing (CC) after steel yielding (Sy) at ultimate load 53.0 and 85.1 kN respectively with 60.6% increase. Consequently, beam S1G failed due to concrete cover splitting (Cs) (**Error! Reference source not found.**-c) at ultimate load of 91.5 kN with 78.7% enhancement over the CB ultimate load.

Moreover, the S1C failed at a load of 96.0 kN due to concrete cover separation (CCs) after Sy (**Error! Reference source not found.**-d) with about 81.1 % load capacity enhancement over the CB and 7.4% over S1G beam. where the high strength of FRP materials ensure higher carrying capacity than that beam strengthened with steel bar. All cracked loads started at the mid-span of all beams then propagated along the beam length. the CCs failure mode caused by formation of shear cracks at the end of the NSM-strengthened bar at load of 80% of the ultimate load. These shear cracks started from the bottom level of the beam up to inner steel reinforcement and then propagated horizontally causing cover separation which is known to be the prevailing failure mode for RC beams reinforced with NSM-FRP bar.

The relation between cracking, yielding and maximum loads of the strengthened beams shown in **Error! Reference source not found.**. All strengthened beams achieved greater yielding loads compared to the conventional beam, while the differences in cracking loads among all the beams tested were minimal. Among the beams reinforced with one steel and GFRP bars, the NSM CFRP strengthened beam exhibited the highest yielding load capacity, whereas the S1G beam recorded the lowest as the three beams (S1S, S1G, and S1C attained yield loads increment by 75.5, 41.8 and 80.0%, respectively over CB. Delaying the yielding load of S1C beam due to the higher stiffness of CFRP bar. After yielding, the NSM FRP strengthened beams exhibited greater stiffness compared to the steel beams, allowing them to achieve a higher load capacity than their steel counterparts (**Error! Reference source not found.**).

Table 3. Results of the experimented tested beams.

Beam	Pcr	δ cr	Py	ζy	δy	Pu	ζu	δu	FM
ID	kN	mm	kN	%	mm	kN	%	Mm	-
CB	13.0	0.7	41.6	--	17.5	53.0	--	125.6	Sy, CC
S1S	15.9	0.7	73.0	75.5	18.8	85.1	60.6	81.2	Sy, CC
S1G	13.4	2.2	59.0	41.8	20.0	94.7	78.7	75.0	Sy, Cs
S1C	14.2	2.0	74.9	80.0	23.4	96.0	81.1	36.3	Sy, CCs

Where:

P_{cr} and δ_{cr} = load and midspan deflection at cracking;
P_y and δ_y = load and midspan deflection at yielding;
ζ_y = % increase in the yielding load,
$\zeta_y = \frac{Py,str-Py,CB}{Py,CB} \times 100$;
P_u and δ_u = load and midspan deflection at ultimate;
ζ_u = % increase in the ultimate load,
$\zeta_u = \frac{Pu,str-Pu,CB}{Pu,CB} \times 100$;
ε_f = maximum strain obtained in the CFRP bar;
ζ_s = strengthening efficiency,
$\zeta_s = \frac{\text{developed strain in the CFRP bar at ultimate load}}{\text{ultimate strain of the CFRP bar}} \times 100$;
FM = failure mode;
CC = concrete crushing;
Cs= concrete cover splitting and
CCs = concrete cover separation

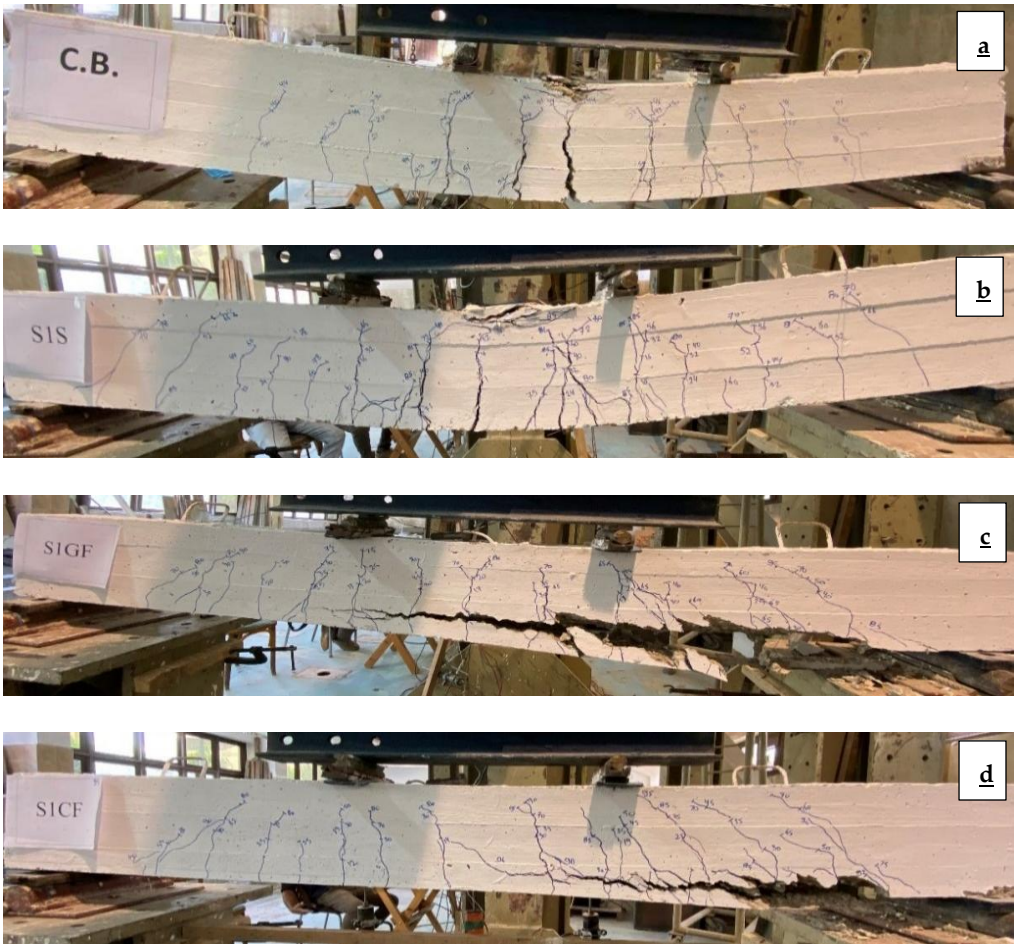

Figure 4. Failure modes and crack behavior of CB and strengthened beams with steel and FRP bars, (a) CB, (b) SIS, (c) SIGF and (d) SICF

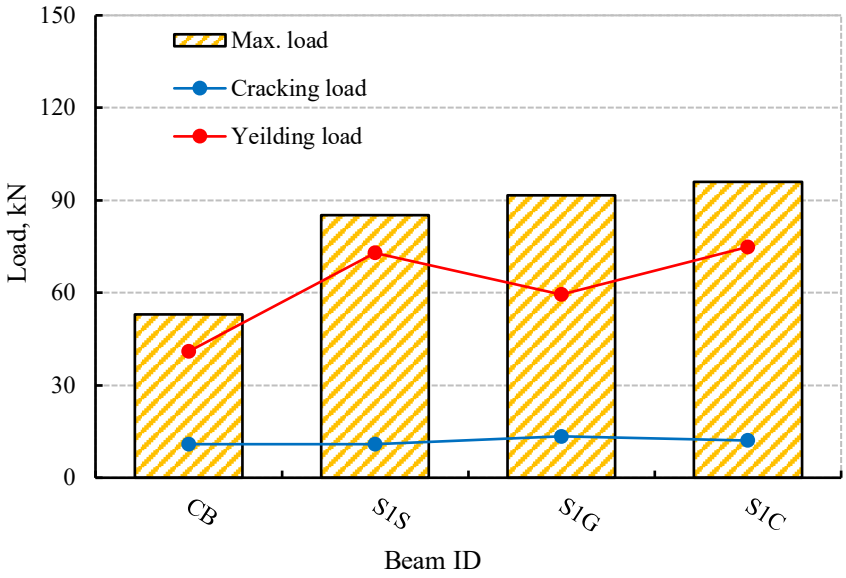

Figure 5. The relation between the trends of cracking, yielding, and maximum loads for the beams

3.3. Load-deflection response and pre-yielding Stiffness of beams

Error! Reference source not found. presents the relationship between the applied load and deflection (P-δ) at the mid-span of the tested beams. The (P-δ) curves divided into three primary phases: the initial linear behavior up to the point of cracking, a linear response from cracking to steel yielding with reduced stiffness, and the phase that begins at steel yielding and continues to the maximum load capacity.

The NSM bars added to the RC beams increased their stiffness, mostly based on the characteristics of the bar materials. When a steel bar was used as the NSM strengthening element, the beam exhibited greater stiffness compared to those reinforced with GFRP or CFRP bars (**Error! Reference source not found.**). After yielding, beams strengthened with FRP NSM bars (CFRP or GFRP) demonstrated higher stiffness than those with steel NSM bars. Since the behavior of the FRP bars remains linear until failure, they maintain their initial stiffness up to that failure, unlike the beams reinforced with NSM steel bars. Consequently, the CFRP NSM strengthened beam displayed the highest stiffness in the P-δ response after the yielding of steel (**Error! Reference source not found.**).

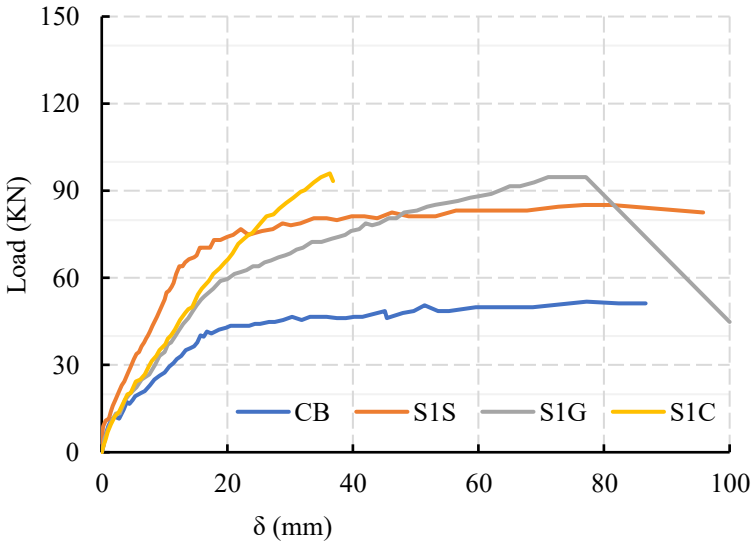

Figure 5. The load-deflection curves of the experimentally tested

The effective pre-yielding stiffness (Ke) was determined for each beam, as shown in **Error! Reference source not found.** and **Error! Reference source not found.**. The pre-yielding stiffness was significantly increased with NSM bars. Compared to the conventional beam (CB), the two beams S1G and S1C achieved an increment in pre-yielding stiffness of 33.28% and 35.2%, respectively. (**Error! Reference source not found.**).

Table 3. Service load, stiffness, energy absorption, and deformability index of RC beams

Beam	Ke	ζ Ke
ID	kN/m	%
C.B	1788.4	--
S1S	3418.5	91.2
S1G	2597.5	45.3
S1C	2936.3	64.2

Ke = effective pre-yield stiffness, $K_e = \frac{Py-Pcr}{\Delta y-\Delta cr} \times 100$

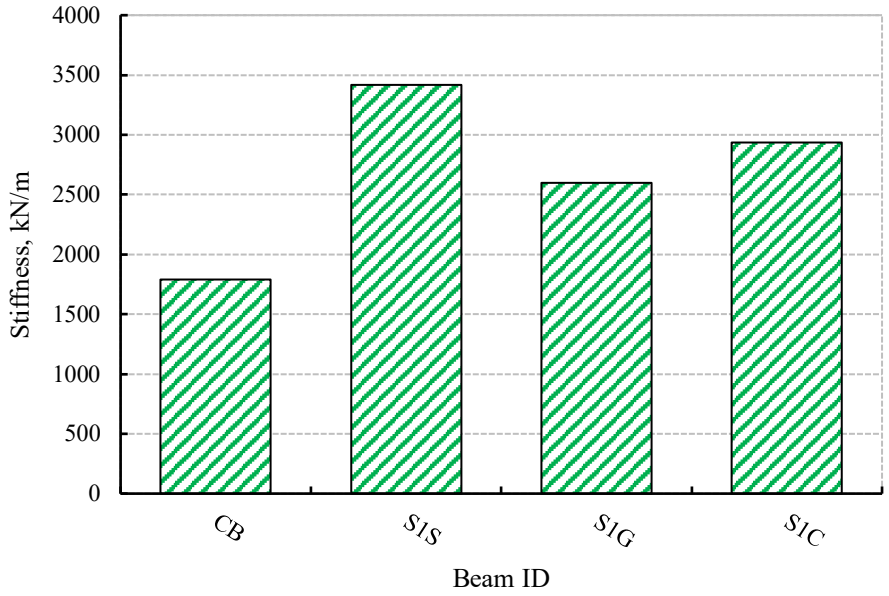

Figure 6. The pre-yielding stiffness of the RC experimentally tested beams

3.3. Load-strain response at the midspan section of the strengthened beams

Generally, the strain increased linearly as the applied force increased until the concrete cracked under tension. When the concrete cracked, all of the tensile stresses it had been carrying were transferred to the tension steel and NSM reinforcement, as the flexural stiffness of the beam decreased the (P-ε) slope also decreased, but until the tension steel yielded, the relationship stayed linear. Following yielding, the beam's flexural stiffness was much decreased, and the slope of the (P-ε) curves also decreased as shown in **Error! Reference source not found.**.

Strengthening using CFRP bar for beam S1C significantly reduced the strain that occurred in the NSM bar compared to GFRP bar for beam S1G as shown in **Error! Reference source not found.**c. This explains the failure of the concrete around the separated concrete cover of the beam S1G.

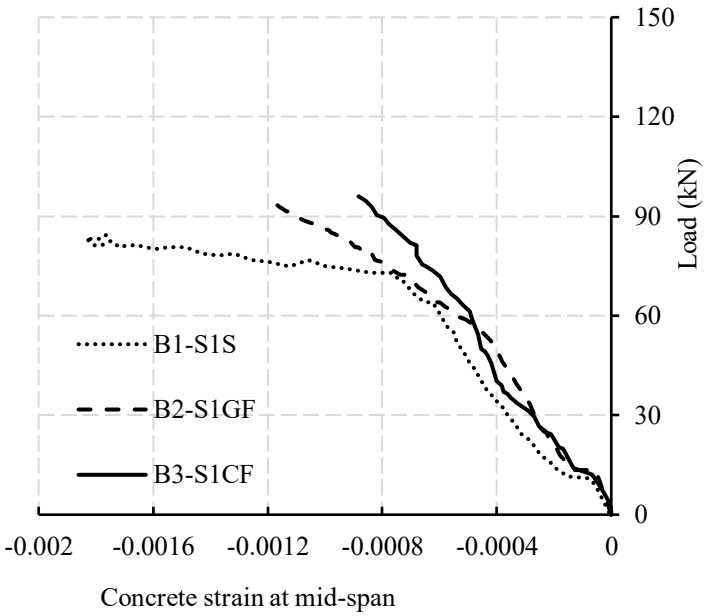

Figure 6. The pre-yielding stiffness of the RC experimentally tested beams

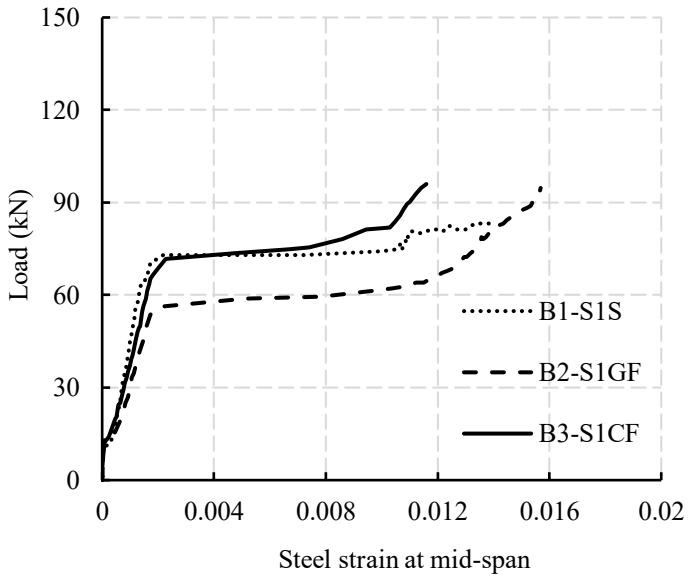

Figure 6. The pre-yielding stiffness of the RC experimentally tested beams

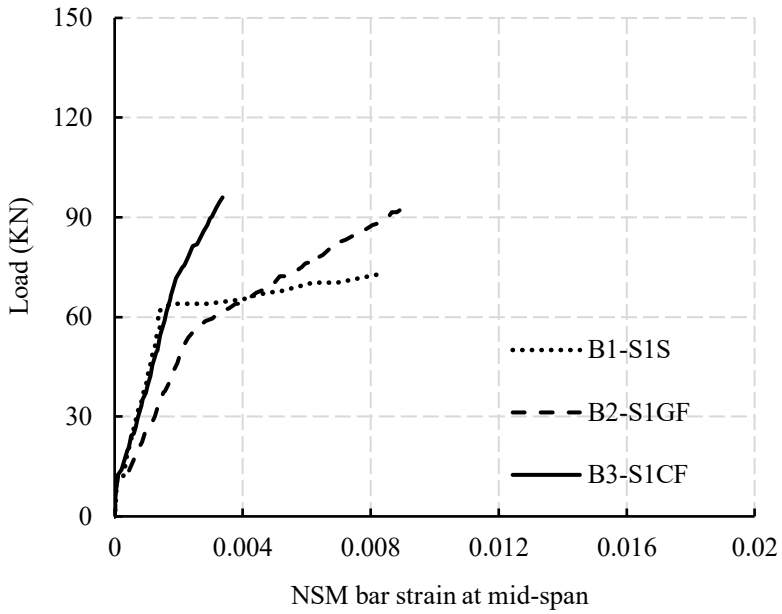

Figure 6. The pre-yielding stiffness of the RC experimentally tested beams

4. Conclusions

Based on the experimental results, the following conclusions could be drawn:

1. For beam strengthened with one steel bar, the NSM bars exhibited lower strain values compared to the internal bars due to their greater axial stiffness. Strengthened with one GFRP bar displayed a nearly linear for the steel one, the NSM bars exhibited lower strain values Conclusions
2. The steel NSM-strengthened RC beams' load capacity increased by roughly 60.6% compared to the CB, while the upgraded RC beams with CFRP and NSM GFRP bars saw increases of roughly 81.1% and 78.7%, respectively. The finding revealed the higher strength of the FRP materials in enhancing the load capacity of the NSM-strengthened compared to steel ones as the failure was governed by the steel yielding in the case of one NSM steel bar and by Cs or CCs for the one NSM GFRP and CFRP bar.
3. The higher stiffness of CFRP bars compared to GFRP bars could delay the yielding of the internal steel, keep the beam stiffness higher than beams with NSM steel and GFRP bars after internal steel yielding, and tend to increase their yielding load capacity. After yielding the NSM FRP strengthened beams had higher stiffness than the steel ones so they could attain higher load capacity than steel ones

Author Contributions: For this research articles with one author, "Conceptualization, A. Ali; methodology, A. Ali.; software, A. Ali.; validation, A. Ali.; formal analysis, A. Ali.; investigation, A. Ali.; resources, A. Ali.; data curation, A. Ali.; writing—original draft preparation, A. Ali.; writing—review and editing, A. Ali.; visualization, A. Ali.; supervision, A. Ali.; project administration, A. Ali.; funding acquisition, A. Ali. Author has read and agreed to the published version of the manuscript."

Funding: This research received no external funding

Data Availability Statement: Data Availability Statement: The original contributions presented in this study are included in the article. Further inquiries can be directed to the corresponding author.

Conflicts of Interest: The authors declare no conflicts of interest.

References

[1] I. Del Prete, A. Bilotta, L. Bisby, and E. Nigro, "Elevated temperature response of RC beams strengthened with NSM FRP bars bonded with cementitious grout," *Compos. Struct.*, vol. 258, p. 113182, 2021, doi: https://doi.org/10.1016/j.compstruct.2020.113182.

[2] A. P. Melinda *et al.*, "Bending performance of laminated veneer lumber timber beams strengthened in the compression side with near-surface mounted CFRP plates," *Case Stud. Constr. Mater.*, vol. 21, p. e03418, 2024, doi: https://doi.org/10.1016/j.cscm.2024.e03418.

[3] S. S. Zhang, "Bond strength model for near-surface mounted (NSM) FRP bonded joints: Effect of concrete edge distance," *Compos. Struct.*, vol. 201, no. June, pp. 664–675, 2018, doi: 10.1016/j.compstruct.2018.06.089.

[4] Y. Ke, S. S. Zhang, M. J. Jedrzejko, G. Lin, W. G. Li, and X. F. Nie, "Strength models of near-surface mounted (NSM) fibre-reinforced polymer (FRP) shear-strengthened RC beams based on machine learning approaches," *Compos. Struct.*, vol. 337, p. 118045, 2024, doi: https://doi.org/10.1016/j.compstruct.2024.118045.

[5] S. Ahmed, I. A. Sharaky, Y. E. Ibrahim, and A. Abdo, "Flexural response of GFRP RC beams strengthened with side and bottom NSM GFRP bars," *Case Stud. Constr. Mater.*, vol. 18, no. October 2022, p. e01858, 2023, doi: 10.1016/j.cscm.2023.e01858.

[6] I. A. Sharaky, S. A. I. Selmy, M. M. El-Attar, and H. E. M. Sallam, "The influence of interaction between NSM and internal reinforcements on the structural behavior of upgrading RC beams," *Compos. Struct.*, vol. 234, p. 111751, 2020, doi: https://doi.org/10.1016/j.compstruct.2019.111751.

[7] X. Li, G. Xing, Z. Chang, and J. Huang, "Experimental and analytical study of RC beams strengthened with prestressed near-surface mounted 7075 aluminum alloy bars," *Structures*, vol. 48, pp. 1693–1706, 2023, doi: https://doi.org/10.1016/j.istruc.2023.01.065.

[8] M. A. Shayanfar, M. Ghanooni-Bagha, and S. Afzali, "Reinforced concrete columns strengthened with near-surface mounted and hybrid FRP under compression with or without eccentricity: Experimental study and finite element modeling," *Case Stud. Constr. Mater.*, vol. 20, p. e02761, 2024, doi: https://doi.org/10.1016/j.cscm.2023.e02761.

[9] ACI440.1R-15, *Guide for the Design and Construction of Structural Concrete Reinforced with Firber-Reinforced Polymer (FRP) Bars*, no. 4. 2015.

[10] A. Bilotta, F. Ceroni, E. Nigro, and M. Pecce, "Efficiency of CFRP NSM strips and EBR plates for flexural strengthening of RC beams and loading pattern influence," *Compos. Struct.*, vol. 124, pp. 163–175, 2015, doi: https://doi.org/10.1016/j.compstruct.2014.12.046.

[11] S. S. Mohamed, O. Hamdy, M. H. Seleem, and I. A. Sharaky, "The flexural behavior and efficiency of RC beams strengthened with SNSM bars under the effect of several end conditions and material properties," *Eng. Struct.*, vol. 308, no. April, p. 117990, 2024, doi: 10.1016/j.engstruct.2024.117990.

[12] M. H. Seleem, F. A. Megahed, A. A. M. Badawy, and I. A. Sharaky, "Performance of NSM and EB methods on the flexural capacity of the RC beams strengthened with reinforced HSC layers," *Structures*, vol. 56, p. 104950, 2023, doi: https://doi.org/10.1016/j.istruc.2023.104950.

[13] F. A. Megahed, M. H. Seleem, A. A. M. Badawy, and I. A. Sharaky, *The flexural response of RC beams strengthened by EB/NSM techniques using FRP and metal materials: a state-of-the-art review*, vol. 8, no. 11. Springer International Publishing, 2023. doi: 10.1007/s41062-023-01245-z.

[14] I. S. Shabana, I. A. Sharaky, A. Khalil, H. S. Hadad, and E. M. Arafa, "Flexural response analysis of passive and active near-surface-mounted joints: experimental and finite element analysis," *Mater. Struct. Constr.*, vol. 51, no. 4, pp. 1–15, 2018, doi: 10.1617/s11527-018-1232-x.

[15] T. M. Elrakib and A. I. Arafa, "Experimental evaluation of the common defects in the execution of reinforced concrete beams under flexural loading," *HBRC J.*, vol. 8, no. 1, pp. 47–57, 2012, doi: 10.1016/j.hbrcj.2012.08.006.

[16] G. D. Airey, "Rheological properties of styrene butadiene styrene polymer modified road bitumens☆," *Fuel*, vol. 82, no. 14, pp.

1709–1719, 2003, doi: https://doi.org/10.1016/S0016-2361(03)00146-7.

[17] "1-s2.0-S2214509525009805-main.pdf."

[18] L. C. Machado, B. L. Damineli, M. S. Rebmann, and S. C. Angulo, "Simple way to model the mechanical properties of concretes with recycled concrete aggregates," *J. Build. Eng.*, vol. 84, p. 108213, 2024, doi: https://doi.org/10.1016/j.jobe.2023.108213.

[19] P. Pan, S. Wu, F. Xiao, L. Pang, and Y. Xiao, "Conductive asphalt concrete: A review on structure design, performance, and practical applications," *J. Intell. Mater. Syst. Struct.*, vol. 26, no. 7, pp. 755–769, 2015, doi: 10.1177/1045389X14530594.

[20] Y. Liang, Z. Ye, F. Vernerey, and Y. Xi, "Development of Processing Methods to Improve Strength of Concrete with 100% Recycled Coarse Aggregate," *J. Mater. Civ. Eng.*, vol. 27, no. 5, pp. 1–9, 2015, doi: 10.1061/(asce)mt.1943-5533.0000909.

[21] S. Xiaoshuang, S. Yanpeng, L. Jinqian, Z. Yuhao, and H. Ruihan, "Preparation and performance optimization of fly ash- slag- red mud based geopolymer mortar: Simplex-centroid experimental design method," *Constr. Build. Mater.*, vol. 450, p. 138573, 2024, doi: https://doi.org/10.1016/j.conbuildmat.2024.138573.

[22] C. qiang Wang, X. yan Lin, M. He, D. Wang, and S. lan Zhang, "Environmental performance, mechanical and microstructure analysis of concrete containing oil-based drilling cuttings pyrolysis residues of shale gas," *J. Hazard. Mater.*, vol. 338, pp. 410–427, 2017, doi: 10.1016/j.jhazmat.2017.05.051.

[23] S. K. Rahman and R. Al-ameri, "A newly developed self-compacting geopolymer concrete under ambient condition," *Constr. Build. Mater.*, vol. 267, p. 121822, 2021, doi: 10.1016/j.conbuildmat.2020.121822.

[24] "nanayakkara2020.pdf."

[25] S. S. Zhang and T. Yu, "Effect of groove spacing on bond strength of near-surface mounted (NSM) bonded joints with multiple FRP strips," *Constr. Build. Mater.*, vol. 155, pp. 103–113, 2017, doi: 10.1016/j.conbuildmat.2017.08.064.

[26] L. Yan, N. Chouw, and K. Jayaraman, "Flax fibre and its composites – A review," *Compos. Part B Eng.*, vol. 56, pp. 296–317, 2014, doi: https://doi.org/10.1016/j.compositesb.2013.08.014.

[27] J. B. Lv, D. J. Lin, B. Fu, S. H. Liu, and Z. J. Han, "Flexural performance of reinforced concrete beams strengthened using near-surface-mounted carbon-fiber-reinforced polymer bars: Effects of bonding patterns," *Compos. Struct.*, vol. 335, no. September 2023, 2024, doi: 10.1016/j.compstruct.2024.117985.

[28] A. A. Shukri, M. A. Hosen, R. Muhamad, and M. Z. Jumaat, "Behaviour of precracked RC beams strengthened using the side-NSM technique," *Constr. Build. Mater.*, vol. 123, pp. 617–626, 2016, doi: https://doi.org/10.1016/j.conbuildmat.2016.07.066.

[29] S. Gong, M. Su, I. Yoshitake, C. Zhu, and H. Peng, "Factors affecting flexural properties of RC beams strengthened with gradually prestressed NSM CFRP strips," *Eng. Struct.*, vol. 306, p. 117865, 2024, doi: https://doi.org/10.1016/j.engstruct.2024.117865.

[30] D. Lau and H. Joen, "Experimental study of hybrid FRP reinforced concrete beams," *Eng. Struct.*, vol. 32, no. 12, pp. 3857–3865, 2010, doi: 10.1016/j.engstruct.2010.08.028.

[31] M. J. Jedrzejko, J. Tian, S. S. Zhang, Y. Ke, X. F. Nie, and Y. M. Yang, "Strengthening of RC beams in shear with novel near-surface mounted (NSM) U-shaped fiber-reinforced polymer (FRP) composites," *Eng. Struct.*, vol. 292, p. 116479, 2023, doi: https://doi.org/10.1016/j.engstruct.2023.116479.

[32] Q. Wang, F. Peng, and Z. Fang, "Slenderness limit for reinforced ultra-high-performance concrete columns," *Adv. Struct. Eng.*, vol. 0, no. 0, p. 13694332241252274, doi: 10.1177/13694332241252274.

[33] T. A. El-Sayed, A. M. Erfan, R. M. Abdelnaby, and M. K. Soliman, "Flexural behavior of HSC beams reinforced by hybrid GFRP bars with steel wires," *Case Stud. Constr. Mater.*, vol. 16, no. February, p. e01054, 2022, doi: 10.1016/j.cscm.2022.e01054.

[34] Z. Sun *et al.*, "Experimental study on the fl exural behavior of concrete beams reinforced with bundled hybrid steel / FRP bars," *Eng. Struct.*, vol. 197, no. July, p. 109443, 2019, doi: 10.1016/j.engstruct.2019.109443.

[35] D. Lau and H. J. Pam, "Experimental study of hybrid FRP reinforced concrete beams," *Eng. Struct.*, vol. 32, no. 12, pp. 3857–3865, 2010, doi: 10.1016/j.engstruct.2010.08.028.

[36] Y. Yang, D. Pan, G. Wu, and D. Cao, "A new design method of the equivalent stress – strain relationship for hybrid (FRP bar and steel bar) reinforced concrete beams," *Compos. Struct.*, vol. 270, no. March, p. 114099, 2021, doi:

10.1016/j.compstruct.2021.114099.

[37] M. Taheri, J. A. O. Barros, and H. Salehian, "Integrated approach for the prediction of crack width and spacing in flexural FRC members with hybrid reinforcement," *Eng. Struct.*, vol. 209, p. 110208, 2020, doi: https://doi.org/10.1016/j.engstruct.2020.110208.

[38] I. A. Sharaky, A. Abdo, and S. Ahmed, "Effect of the NSM material and area on the flexural response of normal strength concrete beams internally reinforced with GFRP and steel bars," *Eng. Struct.*, vol. 292, p. 116565, 2023, doi: https://doi.org/10.1016/j.engstruct.2023.116565.

[39] W. Gang, W. Zhi-Shen, L. Yun-Biao, S. Ze-Yang, and H. Xian-Qi, "Mechanical Properties of Steel-FRP Composite Bar under Uniaxial and Cyclic Tensile Loads," *J. Mater. Civ. Eng.*, vol. 22, no. 10, pp. 1056–1066, Oct. 2010, doi: 10.1061/(ASCE)MT.1943-5533.0000110.

[40] R. Chennareddy and M. M. R. Taha, "Effect of Combining Near-Surface-Mounted and U-Wrap Fiber-Reinforced Polymer Strengthening Techniques on Behavior of Reinforced Concrete Beams," *ACI Struct. J.*, vol. 114, no. 3, pp. 721–730, 2017, doi: 10.14359/51689443.

[41] D. Zhou, Y. Mei, X. Ke, Z. Liu, and W. Xu, "Study on the structural behavior and reinforcement design of openings in subway station floor slabs," *J. Build. Eng.*, vol. 98, p. 110994, 2024, doi: https://doi.org/10.1016/j.jobe.2024.110994.

[42] M. M. A. Kadhim, A. Jawdhari, M. M. Altaee, A. Majdi, and A. Fam, "Parametric investigation of continuous beams strengthened with near surface mounted FRP bars," *Eng. Struct.*, vol. 293, p. 116619, 2023, doi: https://doi.org/10.1016/j.engstruct.2023.116619.

[43] T. Abdelaleem and H. M. A. Diab, "Suggestions for repairing various defects in the NSM strengthening mechanism with hybrid rebars for RC beams: Experimental and numerical study," *Eng. Struct.*, vol. 289, p. 116225, 2023, doi: https://doi.org/10.1016/j.engstruct.2023.116225.

[44] H. M. A. Diab and T. Abdelaleem, "Investigating the efficiency and reliability of different lap-splice configurations in NSM BFRP rods for strengthening RC beams," *Structures*, vol. 65, p. 106697, 2024, doi: https://doi.org/10.1016/j.istruc.2024.106697.